Acta Cryst. (1963). **16**, 589

Structural Changes in Irradiated BeO

By Harry L. Yakel and Bernard Borie

Metals and Ceramics Division, Oak Ridge National Laboratory, Oak Ridge, Tennessee, U.S.A.*

(*Received* 27 *June* 1962)

X-ray diffraction studies of polycrystalline beryllium oxide irradiated to $1{\cdot}5 \times 10^{21}$ nvt ($E_n > 1$ Mev) at 110 °C have shown selective symmetric or asymmetric broadening of reflections $hk{\cdot}l$ with l not zero. Displacements of reflection maxima and centroids occur in such a manner that a unique a_3 lattice parameter cannot be defined from spacing measurements. Models of clustered interstitial and vacancy defects in a damaged BeO lattice have been proposed and the X-ray scattering from these models has been calculated. Comparison of theoretical and experimental results indicates that the best agreement is obtained for an interstitial cluster model. Some physical implications of this model are discussed.

Introduction

Reported investigations of beryllium oxide subjected to pile irradiation have been concerned primarily with changes in macroscopic physical and mechanical properties of polycrystalline compacts (*e.g.*, Elston & Caillat, 1958). However, in a few X-ray diffraction studies of BeO irradiated to fast neutron doses ($E_n > 1$ Mev) of 10^{19} to 10^{20} nvt, only anisotropic expansions of the hexagonal unit cell ($\Delta a_3/a_3 \cong 4-7 \times \Delta a_1/a_1$) have been observed (Bacon & Wilson, 1955; Elston & Caillat, 1958; Clarke *et al.*, 1961). Changes in reflection profiles after irradiation have been noted by Elston & Labbe (1961), but an interpretation of the effect was not given. The anisotropic lattice expansions usually have been attributed to random isolated point defects generated by the fast neutron flux. A general relation between the average lattice expansion and the accumulated neutron dose has been suggested (Clarke *et al.* 1961).

It is the purpose of this paper to report and interpret X-ray diffraction patterns of polycrystalline samples of beryllium oxide irradiated to 10^{21} nvt (fast) at 110 °C. The interpretation will consist of comparisons of the observations with the predicted X-ray scattering from models of radiation-damaged BeO lattices.

Experimental observations

Cylindrical compacts of polycrystalline BeO were prepared by isostatically pressing UOX-grade powder at room temperature, then sintering at 1500 °C in nitrogen. The bulk density of the compacts was 2·7 g.cm^{-3} compared to a theoretical density of 3·01 g.cm^{-3}. Major known metallic impurities were Si 0·011%, Al 0·010%, K 0·010%, Ca 0·005%, Fe 0·002%, and Cr 0·002%. The average grain size in the compacts was about 2μ, although occasional rod-shaped crystals about 100μ in length were present.

The compacts were irradiated in the core of the Engineering Test Reactor in a fast-neutron flux of 3 to 5×10^{14} n.cm^{-2} sec^{-1}. The irradiation temperature of specimens whose diffraction patterns will be considered here was 110 °C and their accumulated fast neutron dose was $1{\cdot}5 \times 10^{21}$ nvt, as measured from ^{54}Mn induced in stainless steel. A general description of changes in macroscopic and microscopic properties produced by irradiation of all compacts has been given elsewhere (Shields *et al.*, 1961).

X-ray diffraction data were obtained from −200 mesh powders prepared by crushing the BeO compacts irradiated at 110 °C, and also from a similar powder of an unirradiated control compact. Data were recorded with standard Debye–Scherrer and diffractometer techniques (Cu $K\alpha$ radiation, $\lambda = 1{\cdot}5418$ Å).

Diffraction patterns from the irradiated material showed a series of unique effects not observed in patterns from specimens irradiated to lower doses at 110 °C or to equivalent doses at high temperature ($T > 500$ °C). These effects may be characterized as follows:

1. $hk{\cdot}0$ reflections were not significantly broadened relative to corresponding reflections from the control specimen. A small expansion of the a_1 lattice parameter was observed (a_1[irr.] $= 2{\cdot}6997 \pm 0{\cdot}0003$ Å).
2. $hk{\cdot}l$ reflections with $l = 2n$ but not 0 were symmetrically broadened relative to the corresponding reflections from the control. The greater the ratio of l^2 to (h^2+k^2+hk), the greater was the observed breadth of the reflection.
3. $hk{\cdot}l$ reflections with $l = 2n+1$ were asymmetrically broadened in such a way that reflection centroids were always at higher 2θ values than the intensity maxima. Again, the greater the ratio of l^2 to (h^2+k^2+hk), the greater was the observed reflection breadth.
4. $hk{\cdot}l$ reflections with $l \neq 0$ were all displaced to lower scattering angles relative to equivalent control reflections. If the a_1 parameter obtained from the $hk{\cdot}0$ reflection spacings was used with the $hk{\cdot}l$ reflection

* Operated by the Union Carbide Corporation for the U.S. Atomic Energy Commission.

spacings (computed at either centroid or maximum intensity positions for $l=2n+1$) to calculate $h_3|\mathbf{b}_3|$ reciprocal lattice spacings, it was found that these spacings were not simple multiples of one another.

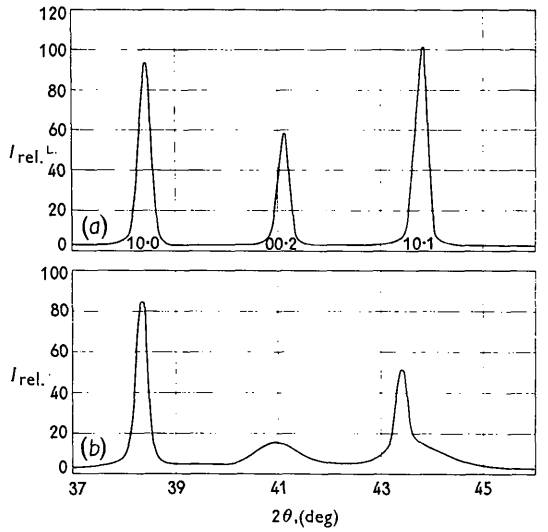

Fig. 1. (*a*) A portion of a Cu $K\alpha$ diffractometer pattern of unirradiated BeO. (*b*) An equivalent portion of a pattern of cold-pressed and sintered *UOX*-grade BeO irradiated to $1{\cdot}5\times10^{21}$ nvt (fast) at 110 °C.

Fig. 1 shows a section of a diffractometer trace over the 10·0, 00·2, and 10·1 reflections which illustrates many of these effects. Also shown is an equivalent section of the pattern from the unirradiated control. A unique a_3 parameter for the irradiated specimen could not be derived from the spacing measurements alone because of effect 4 listed above. Ratios of h_3 values for intensity maxima or centroids of pairs of reflections with l's not zero could be computed, however, and such ratios proved useful in fixing variable parameters for the models of the damaged BeO lattice which will be discussed in the next section.

Models for irradiated BeO

The diffraction effects described above are clearly due to something more than a high density of random isolated point defects. They are similar to those reported for neutron-irradiated graphite by Warren & Chipman (1953) and by Bacon & Warren (1956). The pattern suggests that there is streaking or broadening of reflections along lines in reciprocal space parallel to the $\mathbf{b}_3$ axis, which would be characteristic of some sort of stacking defect in otherwise perfect hexagonal planes. To interpret the pattern, models containing stacking defects were assumed and intensity distributions were computed from them.

Unirradiated BeO has a B4 wurtzite structure below 2000 °C. The hexagonal unit cell ($a_1=2{\cdot}6979$ Å, $a_3=4{\cdot}3772$ Å, Bellamy *et al.*, 1961) contains two formula weights with oxygen atoms at 0, 0, 0 and $\frac{1}{3}, \frac{2}{3}, \frac{1}{2}$ and beryllium atoms at 0, 0, z and $\frac{1}{3}, \frac{2}{3}, z$. Zachariasen (1926) found z to be $\frac{3}{8}$. One may thus represent the structure as two interpenetrating close-packed hexagonal arrays with the usual *ABABABAB* stacking sequence, the two arrays being displaced from each other by $\frac{3}{8}a_3$. If a hexagonal layer of oxygen atoms is represented by the subscript O and that of beryllium by Be, the structure may be described schematically by the sequence

$$A_{\mathrm{O}}A_{\mathrm{Be}}B_{\mathrm{O}}B_{\mathrm{Be}}A_{\mathrm{O}}A_{\mathrm{Be}}B_{\mathrm{O}}B_{\mathrm{Be}}\ldots.$$

The model initially considered presumes that this is also the stacking sequence in the irradiated material except that, at random and with probability α, the spacing between adjacent hexagonal layers is abnormal. There are two ways in which this may be done:

Case (1) $A_{\mathrm{O}}A_{\mathrm{Be}}B_{\mathrm{O}}B_{\mathrm{Be}}A_{\mathrm{O}}/A_{\mathrm{Be}}B_{\mathrm{O}}B_{\mathrm{Be}}\ldots$

Case (2) $A_{\mathrm{O}}A_{\mathrm{Be}}B_{\mathrm{O}}B_{\mathrm{Be}}A_{\mathrm{O}}A_{\mathrm{Be}}/B_{\mathrm{O}}B_{\mathrm{Be}}\ldots.$

The first is more plausible since it disturbs only one of the four Be–O nearest-neighbor distances, while the second disturbs three of them. The following derivation is done for case (1).

Presumably, the cause of such an abnormal spacing is the selective accumulation of debris between two layers. In the following, the small contribution to the intensity associated with this interstitial atomic debris is ignored. For a normal spacing, the distance between nearest-neighbor oxygen layers is $\frac{1}{2}a_3$. For the abnormally expanded spacing, this distance is taken to be $(\frac{1}{2}+\varepsilon)a_3$.

One begins with the usual expression for diffracted intensity in electron units:

$$I=\sum_q\sum_s f_q f_s \exp\left[i\mathbf{k}.(\mathbf{r}_q-\mathbf{r}_s)\right].$$

The position of the qth (or sth) atom, of scattering power f_q, is given by $\mathbf{r}_q$, and $\mathbf{k}=2\pi(h_1\mathbf{b}_1+h_2\mathbf{b}_2+h_3\mathbf{b}_3)$. The vectors $\mathbf{b}_1$, $\mathbf{b}_2$, and $\mathbf{b}_3$ are reciprocal to the unit cell vectors $\mathbf{a}_1$, $\mathbf{a}_2$, and $\mathbf{a}_3$, and h_1, h_2, and h_3 are continuous variables which take on integral values h, k, and l at the reciprocal lattice points.

The position of any atom in the crystal may be written $\mathbf{r}=j\mathbf{a}_1+m\mathbf{a}_2+\delta_n+\mathbf{R}_n$. If the nth hexagonal layer containing the atom is an A layer, $\delta_n=0$; if it is a B layer, $\delta_n=(\mathbf{a}_1-\mathbf{a}_2)/3$. The position coordinate of the nth layer parallel to $\mathbf{a}_3$ is given by the vector $\mathbf{R}_n$; j and m are integers.

For the kind of imperfection considered here, a layer of oxygen atoms is always preceded by a layer of beryllium atoms of opposite stacking sequence and displaced from it by $a_3/8$. Hence if one writes,

$$F_A=f_{\mathrm{O}}+f_{\mathrm{Be}}\exp\left[2\pi i\{(h_1-h_2)/3-h_3/8\}\right],$$

and

$$F_B=f_{\mathrm{O}}+f_{\mathrm{Be}}\exp\left[2\pi i\{(h_2-h_1)/3-h_3/8\}\right],$$

the diffracted intensity may be written

$$I=\sum_j\sum_m\sum_n\sum_{j'}\sum_{m'}\sum_{n'}F_nF_{n'}^{*}\exp\left[2\pi i\{h_1(j-j')+h_2(m-m')\}+i\mathbf{k}.\{\delta_n-\delta_{n'}+\mathbf{R}_n-\mathbf{R}_{n'}\}\right].$$

Here F_n and $F_{n'}$ are either F_A or F_B depending on whether the nth (or n'th) layer is A or B. The summation is performed only over the oxygen atom sites in the crystal.

The summations over j, j', m, and m' may be performed to give

$$\varphi^2 = \frac{\sin^2 \pi N_1 h_1}{\sin^2 \pi h_1} \frac{\sin^2 \pi N_2 h_2}{\sin^2 \pi h_2} ,$$

and the diffracted intensity becomes

$$I = \varphi^2 \sum_n \sum_{n'} F_n F_{n'}^* \exp [i\mathbf{k}.\{\boldsymbol{\delta}_n - \boldsymbol{\delta}_{n'} + \mathbf{R}_n - \mathbf{R}_{n'}\}] .$$

If the number of translation distances in each hexagonal layer (N_1 and N_2) is large, φ^2 is negligibly small except near $h_1 = h$ and $h_2 = k$, where h and k are integers. For a large number of layers (N_3) in the crystal,

$$I = N_3 \varphi^2 \sum_n \langle F_n F_{n'}^* \exp [i\mathbf{k}.(\boldsymbol{\delta}_n - \boldsymbol{\delta}_{n'})] \times \exp [i\mathbf{k}.(\mathbf{R}_n - \mathbf{R}_{n'})] \rangle .$$

If $n - n' = p$ is even,

$$\langle F_n F_{n'}^* \exp [i\mathbf{k}.(\boldsymbol{\delta}_n - \boldsymbol{\delta}_{n'})] \rangle = \tfrac{1}{2}(F_A F_A^* + F_B F_B^*) = f_O^2 + f_{Be}^2 + 2 f_O f_{Be} \cos 2\pi \left(\frac{h-k}{3}\right) \cos 2\pi \frac{h_3}{8} = G .$$

If p is odd,

$$\langle F_n F_{n'}^* \exp [i\mathbf{k}.(\boldsymbol{\delta}_n - \boldsymbol{\delta}_{n'})] \rangle = \tfrac{1}{2}\left(F_A F_B^* \exp\left[2\pi i \left(\frac{k-h}{3}\right)\right] + F_B F_A^* \exp\left[2\pi i \left(\frac{h-k}{3}\right)\right]\right) = (f_O^2 + f_{Be}^2) \cos 2\pi \left(\frac{h-k}{3}\right) + 2 f_O f_{Be} \cos 2\pi \frac{h_3}{8} = J .$$

With $\mathbf{R}_p = \mathbf{R}_n - \mathbf{R}_{n'}$, the diffracted intensity may be written

$$I = N_3 \varphi^2 \{G \sum_{p \text{ even}} \langle \exp [i\mathbf{k}.\mathbf{R}_p] \rangle + J \sum_{p \text{ odd}} \langle \exp [i\mathbf{k}.\mathbf{R}_p] \rangle\} .$$

With random layer defects, the Mering relation (1949) may be used:

$$\langle \exp [i\mathbf{k}.\mathbf{R}_{\pm p}] \rangle = \langle \exp [i\mathbf{k}.\mathbf{R}_{\pm 1}) \rangle^{|p|} .$$

For positive p,

$$\langle \exp [i\mathbf{k}.\mathbf{R}_{+1}] \rangle = (1 - \alpha + \alpha \exp [2\pi i h_3 \varepsilon]) \exp [\pi i h_3] ,$$

and for negative p,

$$\langle \exp [i\mathbf{k}.\mathbf{R}_{-1}] \rangle = (1 - \alpha + \alpha \exp [-2\pi i h_3 \varepsilon]) \times \exp [-\pi i h_3] .$$

When $h - k$ is a multiple of three, let $I = I_1(h_3)$. Then

$$G = J = f_O^2 + f_{Be}^2 + 2 f_O f_{Be} \cos 2\pi \frac{h_3}{8} ,$$

and

$$I_1(h_3) = N_3 \varphi^2 \left(f_O^2 + f_{Be}^2 + 2 f_O f_{Be} \cos 2\pi \frac{h_3}{8}\right) \times \sum_p \langle \exp [i\mathbf{k}.\mathbf{R}_p] \rangle .$$

If $\beta \exp [i\gamma] = (1 - \alpha + \alpha \exp [2\pi i h_3 \varepsilon]) \exp [\pi i h_3]$, then

$$\sum_p \langle \exp [i\mathbf{k}.\mathbf{R}_p] \rangle = \sum_p \beta^{|p|} \exp [ip\gamma] = (1 - \beta^2)/(1 - 2\beta \cos \gamma + \beta^2)$$

and

$$I_1(h_3) = N_3 \varphi^2 \left(f_O^2 + f_{Be}^2 + 2 f_O f_{Be} \cos 2\pi \frac{h_3}{8}\right) \times \{(1 - \beta^2)/(1 - 2\beta \cos \gamma + \beta^2)\} . \quad (1)$$

By a similar derivation, one may show that $I_2(h_3)$, the diffracted intensity in the case that $h - k$ is not a multiple of three, is given by

$$I_2(h_3) = I_1 \left\{\frac{\beta \cos \gamma}{1 + 2\beta \cos \gamma + \beta^2}\right\} + N_3 \varphi^2 \left(f_O^2 + f_{Be}^2 - f_O f_{Be} \cos 2\pi \frac{h_3}{8}\right) \left\{\frac{1 - \beta^2}{1 + 2\beta \cos \gamma + \beta^2}\right\} . \quad (2)$$

Comparisons of predicted and observed scattering

With the aid of an IBM 7090 computer, the line contours predicted by equations (1) and (2) were determined for the following ranges of the variables: $0 < h_3 \leq 4{\cdot}5$; $0 < \alpha \leq 0{\cdot}25$; and $0 < \varepsilon < 0{\cdot}8$. For these calculations, f_{Be} was taken to be $\frac{1}{2} f_O$, and the quantity computed was $I/(N_3 \varphi^2 f_O^2)$. The results were projected onto radial lines in reciprocal spaces so that the contours could be directly compared to those experimentally observed in the powder pattern. It was found that the model predicts line broadenings, shifts, and asymmetries critically dependent on $hk{\cdot}l$, α, and ε. Quantitative agreement with experiment was found only for ε between 0·36 and 0·40 and for α between 0·05 and 0·10.

The intensity distribution was also computed for a model based on case (2) described above, in which three of the four Be–O nearest-neighbor bonds are disturbed by an expanded spacing. For the same ranges of α and ε used above, no agreement with experiment could be found.

An effort was also made to reproduce the ex-

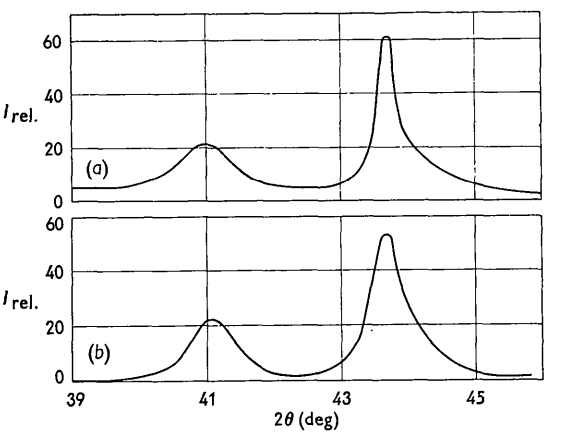

Fig. 2. 00·2 and 10·1 reflection profiles for irradiated BeO, (*a*) As-observed, and (*b*) As-calculated for $\varepsilon = 0{\cdot}40$, $\alpha = 0{\cdot}05$.

perimental observations by assuming that random hexagonal layers contained an abnormally high vacancy concentration, and that the interlayer spacing on either side of such a layer is anomalously contracted. Only symmetrically broadened reflections were found for this model, and it was abandoned.

The interstitial cluster model, case (1), adequately reproduces both the shapes and positions of the Bragg maxima at small scattering angles, as shown in Fig. 2. However, at large 2θ, though the reflection position and direction of asymmetry are correctly given by the model, the experimentally observed lines are significantly broader. It seemed that a likely explanation for this is that a range of ε values exists in the damaged crystal, rather than a single unique value as assumed in the model. The quantity of atomic debris causing an expanded spacing should determine ε, and this clearly need not be the same for all such planes. The extra strain broadening associated with this effect should be apparent far from the origin in reciprocal space, but should make little difference at small scattering angles.

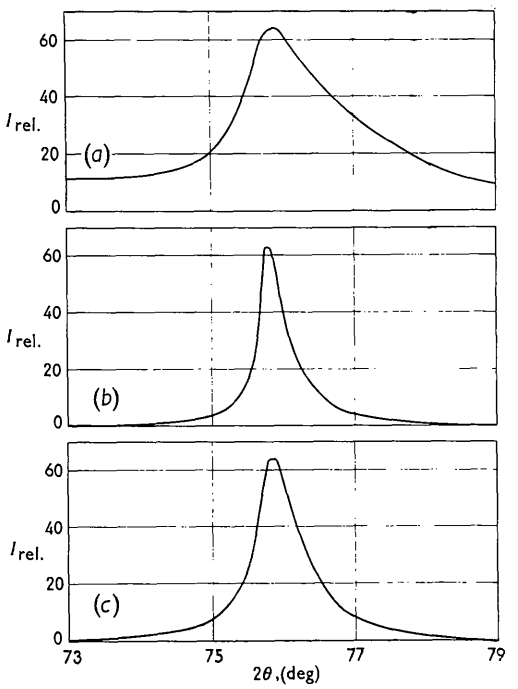

Fig. 3. 10·3 reflection profiles for irradiated BeO, (*a*) As-observed; and As-calculated for (*b*) $\varepsilon_0=0{\cdot}40$, $\alpha=0{\cdot}10$, $\frac{1}{2}\Delta\varepsilon=0{\cdot}0$, and (*c*) $\varepsilon_0=0{\cdot}40$, $\alpha=0{\cdot}05$, $\frac{1}{2}\Delta\varepsilon=0{\cdot}08$.

It is straightforward to modify the diffraction theory to allow for a distribution of ε's. This was done both for square and Gaussian distributions. Substantially the same result was found in both cases. Negligibly small changes in the line positions resulted, and the line widths in the low-angle region were unaffected. However, at large 2θ, as expected, a substantial increase in line widths was found. This is illustrated in Fig. 3 for $hk{\cdot}l=10{\cdot}3$. A distribution of spacing expansions also seems to cause a small decrease in the degree of asymmetry.

Finally, the theoretical h_3 values at which $hk{\cdot}l(l\neq 0)$ intensity maxima or centroids occur for acceptable ε and α values may be combined with the experimentally observed positions of these maxima or centroids to give a value for $\frac{1}{2}a_3$, the normal interlayer spacing in the irradiated structure when an interstitial cluster is not present. This value is $2{\cdot}22\pm 0{\cdot}01$ Å, which is 1·3% larger than the spacing characteristic of unirradiated BeO.

Discussion

From the comparisons presented in the preceding section, it is evident that the predicted X-ray scattering from the interstitial cluster model, case (1), reproduces most of the observed diffraction effects from the irradiated BeO specimens considered here. Best agreement is obtained for a probability, α, of 0·05 to 0·10 with expansion parameters ε distributed about a mean ε_0 of 0·36 to 0·40 in a Gaussian or square distribution of half-width 0·04 to 0·08. Some of the physical implications of these results may now be considered.

It has been assumed that the interlayer expansions are due to clusters of interstitial defects. Not all defects are clustered, however, since the normal interlayer spacings are also expanded by 1·3% relative to the undamaged lattice. If this expansion is attributed to residual isolated defects, their concentration may be estimated as 0·4% through a relation developed by Kinchin & Pease (1955). The fractional number of all displaced atoms (in clusters or isolated) may be estimated from the experimental dose, an average cross section, and the number of displacements per primary knock-on. An assumed average cross section of 2·5 barns for Be and O, with about 14 displacements per primary (Sabine, Pryor & Hickman, 1961), gives $N_d/N\cong 5\%$ for a $1{\cdot}5\times 10^{21}$ nvt (fast) dose. If some allowance is made for in-pile annealing, it would seem that roughly 90% of the interstitial defects are in clusters while about 10% remain as isolated point defects.

The values of ε_0, α, and $\frac{1}{2}\Delta\varepsilon$ for which the predicted X-ray scattering most closely approximates that observed do not lead to any significant conclusions about the nature of the atoms in the clusters. ε_0 is near 0·4, so that a cluster has almost the same thickness as a normal lattice layer. Monatomic layers of oxygen atoms or ions, diatomic layers of beryllium atoms or ions* or of helium atoms produced by an

* A possible condensation of beryllium interstitials in the clusters during postirradiation annealing was considered. This could produce platelets of metallic beryllium, in analogy to the formation of metallic lithium in irradiated LiF (Lambert & Guinier, 1958). Annealed specimens failed to produce diffraction effects attributable to metallic beryllium, however, and a simple recovery of the lattice to its unirradiated condition was observed.

$(n, 2n)$ reaction with Be, or various combinations of these are all possible and consistent with the deduced parameters.

The abnormally expanded interlayer spacings of the interstitial cluster model, case (1), have been assumed to occur at random. This is a departure from the model proposed for irradiated graphite (Warren & Chipman, 1953), where a pseudo-regular array of interstitial clusters had to be assumed in order to predict the observed asymmetric broadening of the basal plane reflections. This regularity was attributed to a tendency for clusters to avoid being close neighbors, and it was concluded that the clusters in irradiated graphite must be small in area. If the clusters in the irradiated BeO specimens considered here are random, the argument of Warren & Chipman could be inverted to suggest that the clusters have a relatively large area. To place quantitative values on these 'small' and 'large' areas is beyond the capability of the available data for either graphite or BeO.

A relation, given by Warren & Chipman, between the lateral radius of a cluster, r, the fraction of interstitial clusters per atom, N_i/N, and the average area per atom in a layer, ϱ, is $\pi r^2(N_i/N) = \alpha\varrho$ where α is the cluster probability parameter as used above. If the area of the cluster is about equal to the sum of the areas of the atoms in the cluster and there are n atoms in the average cluster, $n\varrho(N_i/N) \cong \alpha\varrho$, or $n(N_i/N) \cong \alpha$. But $n(N_i/N)$ is just the fractional number of displaced atoms in clusters which, for the conditions of this experiment, is about 4%. The best value of α agrees with this within a factor of 2 to 2·5.

Experimental verifications of defect clusters in irradiated solids have been reported recently. It has been suggested by Barnes & Mazey (1960) and by Makin, Whapham & Minter (1961) that the large clusters observed through electron microscopy of neutron-irradiated copper should be interstitial in nature while smaller clusters have been identified with multiple vacancies. Long wavelength neutron scattering from irradiated BeO has indicated the existence of interstitial and/or vacancy clusters (Sabine, Pryor & Hickman, 1961), and direct electron microscopic observations of large defect clusters in the same material have been reported recently (Clarke, 1962).

Conclusions

The following conclusions can be drawn from the work reported here:

1. Unique X-ray diffraction effects involving selective reflection broadening and displacement have been observed in a polycrystalline, cold-pressed and sintered specimen of UOX-grade BeO irradiated to $1{\cdot}5 \times 10^{21}$ nvt (fast) at 110 °C.

2. These observations are reproduced by a model of the damaged BeO lattice in which interstitial clusters expand random spacings between close-packed Be–O layers normal to the hexad axis. They are not reproduced by a model containing only vacancy clusters.

3. Abnormally expanded interlayer spacings have magnitudes $(\frac{1}{2} + \varepsilon)a_3$, where ε values are distributed about a mean ε_0, and occur with a probability α. An ε_0 of 0·36 to 0·40, a distribution half-width of 0·04 to 0·08, and a probability of 0·05 to 0·10 give the best agreement between predicted and observed X-ray scattering. a_3 is computed to be $4{\cdot}44 \pm 0{\cdot}02$ Å.

4. Information about the nature of the atoms in interstitial clusters and about the lateral areas of the clusters is not directly available from the data. The derived value of α is in fair agreement with the number of atoms displaced by the neutron flux which are not present as isolated defects.

The authors gratefully acknowledge the co-operation and interest of the Reactor Chemistry Division of the Oak Ridge National Laboratory. In particular, thanks are due to G. M. Watson, W. E. Browning, Jr., G. W. Keilholtz, J. E. Lee, and R. P. Shields. R. M. Steele of the Metals and Ceramics Division made many of the diffraction pattern measurements. Programming of the intensity calculation was possible through the assistance of R. D. Ellison and H. A. Levy of the Chemistry Division.

References

Bacon, G. E. & Wilson, S. A. (1955). *Acta Cryst.* **8**, 844.
Bacon, G. E. & Warren, B. E. (1956). *Acta Cryst.* **9**, 1029.
Barnes, R. S. & Mazey, D. J. (1960). *Phil. Mag.* **5**, 1247.
Bellamy, B., Baker, T. W. & Livey, D. T. (1961). AERE-R-3774.
Clarke, F. J. P., Tappin, G. & Ghosh, T. K. (1961). AERE-R-3749, Part II.
Clarke, F. J. P. (1962). AERE-R-3971.
Elston, J. & Caillat, R. (1958). *Proceedings of the Second United Nations International Conference on the Peaceful Uses of Atomic Energy*, Vol. 5, p. 345. Geneva, U.N.
Elston, J. & Labbe, C. (1961). *J. Nuclear Materials*, **4**, 143.
Kinchin, G. H. & Pease, R. S. (1955). *Rep. Progr. Phys.* **18**, 1.
Lambert, M. & Guinier, A. (1958). *C. R. Acad. Sci. Paris*, **246**, 1678.
Makin, M. J., Whapham, A. D. & Minter, F. J. (1961). AERE-R-3770.
Mering, J. (1949). *Acta Cryst.* **2**, 391.
Sabine, T. M., Pryor, A. W. & Hickman, B. S. (1961). *Nature, Lond.* **191**, 1385.
Shields, R. P., Lee, J. E., Jr. & Browning, W. E., Jr. (1961). Abstracts of the Winter Meeting, American Nuclear Society, Chicago, Illinois.
Warren, B. E. & Chipman, D. R. (1953). KAPL-938, declassified.
Zachariasen, W. H. (1926). *Z. phys. Chem.* **119**, 201.